Bismuth Titanates /TiO_2 Heterostructures and Nanosheets: Fabrication and High Visible Light Photocatalytic Activity on Acid Blue 1 Dye

Shang-Yi Chou (周尚毅), Yong-Ming Dai(戴永銘), Wei-Chieh Lin (林暐傑), Shie-Ru Tsai (蔡協儒), Chiing-Chang Chen (陳錦章)*

Department of Science Application and Dissemination, National Taichung University of Education

*Email: ccchen@mail.ntcu.edu.tw

Abstract

In this paper, a facile one-step synthesis route using hydrothermal technique has been prepared for the exploitation of $Bi_{12}TiO_{20}$ / $Bi_4Ti_3O_{12}$ / TiO_2, $Bi_{12}TiO_{20}$ / $Bi_2Ti_2O_7$ / TiO_2, and $Bi_4Ti_3O_{12}$ / $Bi_2Ti_4O_{11}$ /TiO_2 heterostructures. Besides, a pure phase bismuth titanates, $Bi_4Ti_3O_{12}$ and $Bi_2Ti_2O_7$ nanosheets, have also been prepared by using same methods. The samples are characterized by XRD, FE-SEM-EDS, HR-XPS, FT-IR, BET, and DRS. UV-Vis spectra show heterostructures and nanosheets materials to be indirect semiconductors with an optical bandgap of 2.54-3.06 eV at 90^oC and 2.54-2.73 eV at 140-240 ^oC for 12-72 h, respectively. The thickness of the as-grown nanosheets is about 20 nm and the size of the nanosheets increases with the increase of hydrothermal temperature. Photocatalytic tests display that these heterostructures and bismuth titanates possess a much higher degradation rate of acid blue 1 (AB1) than the P25-TiO_2 under visible light. The enhanced photocatalytic activity can be attributed to the effective separation of photogenerated carriers driven by the photoinduced potential difference generated at these heterostructures interface, and the extended absorption in the visible light region resulting from the $Bi_4Ti_3O_{12}$ and $Bi_2Ti_2O_7$ nanosheets. This is the first study showing the superior activities of $Bi_{12}TiO_{20}$ / $Bi_4Ti_3O_{12}$ / TiO_2, $Bi_{12}TiO_{20}$ / $Bi_2Ti_2O_7$ / TiO_2, and $Bi_4Ti_3O_{12}$ / $Bi_2Ti_4O_{11}$ / TiO_2 heterostructures as a promising visible-light-responsive photocatalyst. In order to obtain a better understanding on the mechanistic details of the bismuth titanate-assisted photodegradation of the AB1 dye under visible irradiation, the intermediates of the process are separated, identified and characterized by HPLC-ESI-MS technique in the study.

NSC Project no. : NSC 99-2113-M-142-001-MY2

Keywords: Bismuth titanates, Heterostructure, Nanosheet, visible-light-responsive Photocatalyst, hydrothermal

1 Introduction

Among all the photocatalysts, TiO_2 attracts the most attention because of its high chemical stability, inexpensive cost, and mild effect on the environment. Its applications include self-cleaning [1], production of new energy [2], and degradation of harmful materials [3]. However, the band gap of TiO_2 is 3.2 eV that it absorbs only the ultraviolet light ($\lambda < 400$ nm), which only accounts for about 4% of the sunlight [4]. The reactivity and selectivity are still not enough for large-scale applications. It is of interest to find new photocatalytic materials with higher catalytic activity for the photocatalytic methods to develop a viable method for solving both environmental and energy problems in the future. Recently, Bismuth Titanates/TiO_2 have received more attention because of its unique crystal structure and higher activity, compared with TiO_2 catalysts [5-7]. The crystal structures of Bismuth Titanates/TiO_2 are comprised of Ti–O octahedra units and Bi–O tetrahedra units. Because Bismuth Titanates/TiO_2 crystals have the characteristic structures of octahedral TiO_6 units, it is of interest to

examine the photochemical properties of the crystals. Photocatalytic properties of Bismuth Titanates/TiO_2 have been examined before. Yao et al. reported that Bismuth Titanates/TiO_2 crystals exhibited high photocatalytic activity towards photodegradation of methyl orange under UV-light [8].

Thus, it is still a challenge to find a novel and simple synthetic route for Bismuth Titanates/TiO_2 nanoscaled materials. In this study, we report a facile way to synthesize Bismuth Titanates/TiO_2 through a hydrothermal method using $Bi(NO_3)_3$•$5H_2O$ as the precursor at 90 and 190 ℃ under atmospheric pressure for the first time. During the synthesis process, NaOH is used as the transformation agent. The photocatalytic activity of as-prepared Bismuth Titanates/TiO_2 is evaluated for the elimination of acid blue 1 (AB1).

2 Experiment

2.1 Materials and Preparations

The experimental procedure was described as followed. At first, appropriate amounts of $Bi(NO_3)_3$ • 5H2O and P-25 (molar rate of Bi /Ti=1, 2/3, 4/3, and 12) were dissolved into NaOH solution. Finally, the mixed solution was transferred into a stainless steel autoclave. The autoclave was heated to 190℃ and kept for 24 h, and then cooled down to room temperature. $Bi(NO_3)_3$ • $5H_2O$ and P-25 (molar rate of Bi /Ti=12) were dissolved into NaOH solution (with various concentration 1M, 2.5M, 5M, and 10M) by being heated the solution at 90℃ for 24 h, and then cooled to room temperature. All the products were filtered and washed with distilled water several times until pH value close to 7 again, and dried at 60℃ for 12 hrs. The samples are listed in Table 1.

Table 1: Bismuth titanate obtained under different reaction conditions.

Samples	$Bi(NO_3)$	TiO_2	NaOH	Temperature	Time
	(mmol)	(mmol)	(M)	(℃)	(h)
B1T1-2.5-190-24	1	1	2.5	190	24
B2T3-2.5-190-24	2	3	2.5	190	24
B4T3-2.5-190-24	4	3	2.5	190	24
B12T1-2.5-190-24	12	1	2.5	190	24
B12T1-1-90-24	12	1	1	90	24
B12T1-2.5-90-24	12	1	2.5	90	24
B12T1-5-90-24	12	1	2	90	24
B12T1-10-90-24	12	1	10	90	24

2.2 Characterization

The precipitates were further characterized. Powder X-ray diffraction (XRD) was performed on a MAC Sience, MXP18 X-ray diffractometer with Cu Kα radiation, and operated at 40 kV and 80 mA. FE-SEM-EDS measurements were carried out with a field-emission microscope (JEOL JSM-7401F) at an acceleration voltage of 15 kV, and an HRXPS measurement was carried out with ULVAC-PHI XPS. The Al Kα radiation was generated with a voltage of 15 kV. Absorption measurements were carried out by using a Shimadzu UV-2100S spectrophotometer. The BET specific surface areas of the samples were measured with an automatic system (Micromeritics Gemini 237 ◦C) using nitrogen gas as the adsorbate, at liquid nitrogen temperature. The HPLC-PDA-ESI-MS system consisted of a Waters 1525 binary pump, a 2998 photodiode array detector, and a 717 plus autosampler. Besides, a ZQ2000 micromass detector and an Atlantis TM C18 column (250 mm × 4.6 mm i.d., dp = 5 μm) were used for separation and identification. The column effluent was introduced into the ESI source of the mass spectrometer

2.3 Photocatalytic reaction

Photocatalytic activities of bismuth titanate were studied by the degradation of CV under visible light irradiation of a 20 watt lamp. An average irradiation intensity of 5.2 W/m^2 was maintained throughout the experiments and measured by the internal radiometer. Aqueous dispensions of CV (100 ml, 10 ppm) and the given amount of catalyst powder were placed in a Pyrex flask. The pH value of the dispensions was adjusted by adding either NaOH or HNO_3 solutions. Before irradiation, the dispensions were magnetically stirred in the dark for 30 min to reach an adsorption/desorption equilibrium between the dye and the surface of the catalyst under ambient air-equilibrated conditions. At the given irradiation time intervals, 5 ml aliquot was collected and centrifuged to remove the catalyst. The supernatant was analyzed by HPLC-ESI-MS after readjusting the chromatographic conditions in order to make the mobile phase compatible with the working conditions of the mass spectrometer.

3 Results and Discussion

3.1 Characterizations of as-prepared powder

The XRD patterns of the prepared bismuth titanateunder different Bi/Ti mole ratios are shown in Figure 1 (a). When the Bi/Ti mole ratio was 1, the diffraction peaks of P-25 were observed. With an increase of the Bi/Ti ratio, the diffraction peaks of $Bi_4Ti_3O_{12}$ became clear. When the Bi/Ti ratio increased to 12, the heights of the diffraction peaks belonging to $Bi_{12}TiO_{20}$ / $Bi_4Ti_3O_{12}$ / TiO_2 increased further. Compared with the previous Bi/Ti ratio, the developed hydrothermal process successfully increased the Bi/Ti ratio of $Bi_{12}TiO_{20}$/$Bi_4Ti_3O_{12}$ / TiO_2 from 1 to 12.

Figure 1 (b) shows X-ray diffraction data for bismuth titanate samples prepared at different NaOH concentration from 1M, 2.5M, 5M to 10M for 90°C and 24 h, respectively. With an increase of reaction temperature, the diffraction peaks of $Bi_{12}TiO_{20}$ / $Bi_4Ti_3O_{12}$ / TiO_2 became clear. When NaOH concentration increased to 10M, the heights of the diffraction peaks belonging to $Bi_{12}TiO_{20}$ / $Bi_4Ti_3O_{12}$ / TiO_2 increased further, while full-width at half-maximum of all peaks decreased. It revealed that bismuth titanate with well crystallinity was synthesized at higher NaOH concentration. All diffraction peaks were assigned to $Bi_{12}TiO_{20}$ / $Bi_4Ti_3O_{12}$ / TiO_2 as reported in JCPDS file [9-11], indicating that the synthesized was bismuth titanate.

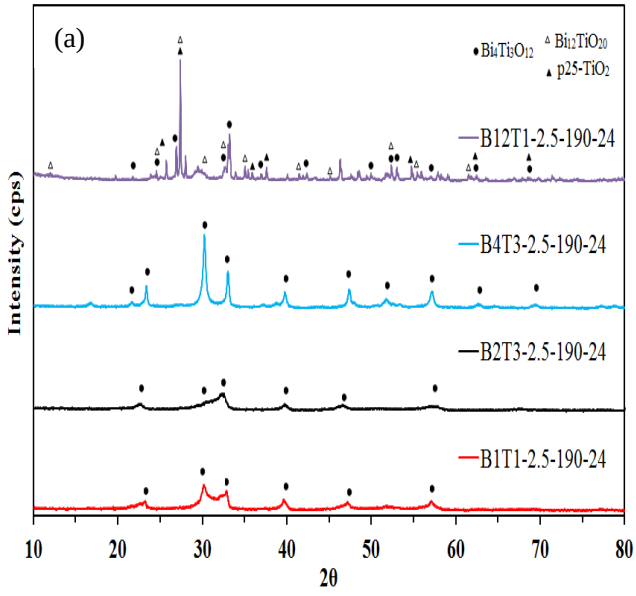

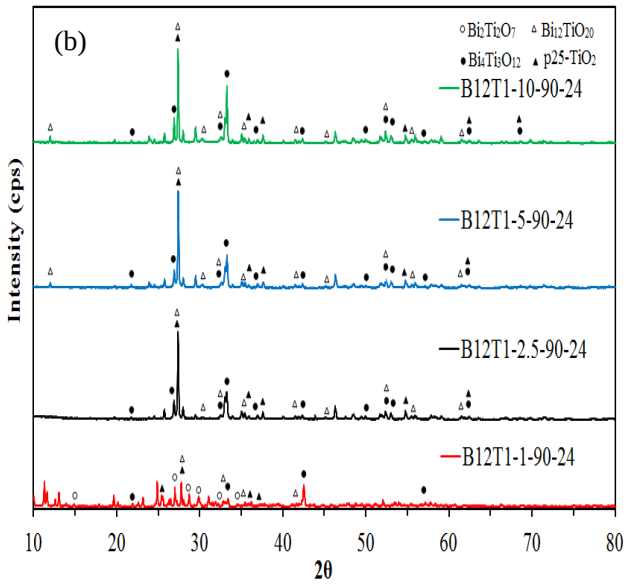

Figure 1: XRD patterns of as-prepared under different (a), Bi/Ti mole ratios and, (b) NaOH concentration.

Bismuth titanate was prepared with $Bi(NO_3)_3$•$5H_2O$ and P-25 by the hydrothermal method at 190 °C for the Bi/Ti mole ratios 1, 2/3, 4/3, and 12. The surface morphology of the photocatalysts was examined by FE-SEM (Figure 2). Figure 2, were the Bismuth titanate powder, showing that the bismuth titanate powder synthesized were composed of nano-sized particles, which were about 20 nm in size, and that each particle was nearly square in shape and dense in density. Then, the bismuth titanate became to form irregular nanoplates above the Bi/Ti mole ratio 4/3, and the agglomerate nanosheet shape increased with further increasing Bi/Ti mole ratio up to 12. The morphology of the bismuth titanate as a function of NaOH concentration was directly monitored by FESEM, as shown in Figure 3. The FE-SEM results indicated that the bismuth titanate surface started to become rough and form nanoscale particles above 2.5M NaOH concentration, and the agglomerate nanoplates increased with further increasing NaOH concentration up to 10M.

The UV–vis adsorption spectra of synthesized catalysts are shown in Figure 4. UV–vis adsorption spectra of the prepared bismuth titanate under different Bi/Ti mole ratios are shown in the inset of Figure 4(a). Their corresponding band gap energies were calculated, which were close to 2.65-3.11 eV. The B12T1-2.5-190-24 had good visible light absorption with band gap energy Eg =

2.65 eV.

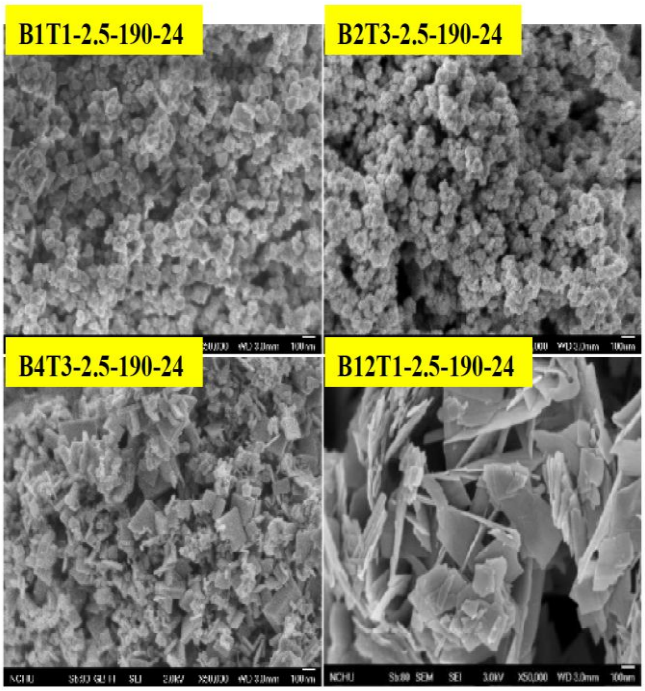

Figure 2: FE-SEM images of the nanosheets bismuth titanate prepared by the hydrothermal autoclave method at 190 ˚C, 24 h; for Bi/Ti mole ratio = 1 (a), 2//3 (b), 4/3 (c), and 12 (d)

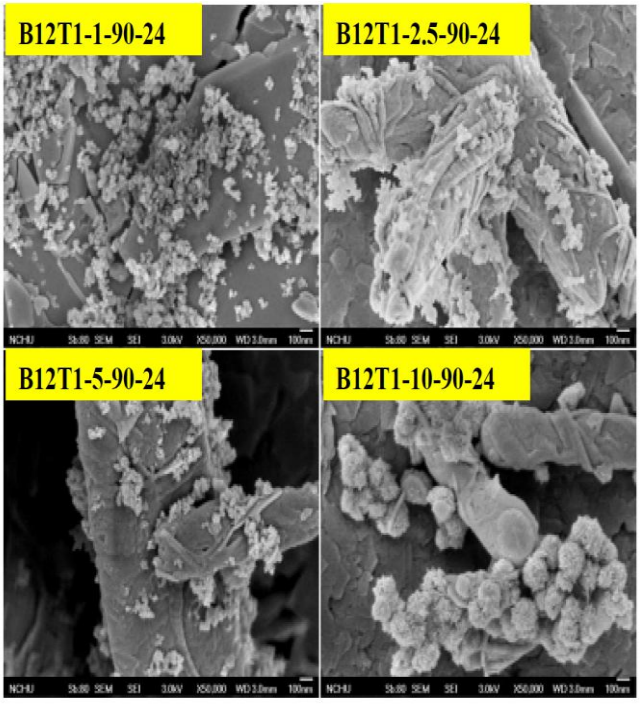

Figure 3: FE-SEM images of the nanosheets bismuth titanate prepared by the hydrothermal autoclave method at 90 ˚C, 24 h; for NaOH concentrations = 1 (a), 2.5 (b), 5 (c), and 10 (d)

Clearly, the onset of the absorption edge shifted to higher wavelengths as the Bi/Ti mole ratio increased. A close relationship existed between this absorption and the amount of Bi incorporated in the bismuth titanate. Figure 4 (b) shows UV–vis adsorption spectra data for bismuth titanate samples prepared at different NaOH concentration. Their corresponding band gap energies were calculated, which were close to 2.67-3.06eV. The B12T1-10-90-24 had good visible light absorption with the band gap energy Eg = 2.65 eV. In our hydrothermal process, NaOH played a significant role in the formation of bismuth titanate nanocrystals. Different types of unidentified products were formed when using different NaOH concentration. Further investigation on the effect of NaOH on the formation of bismuth titanate nanocrystals is in progress.

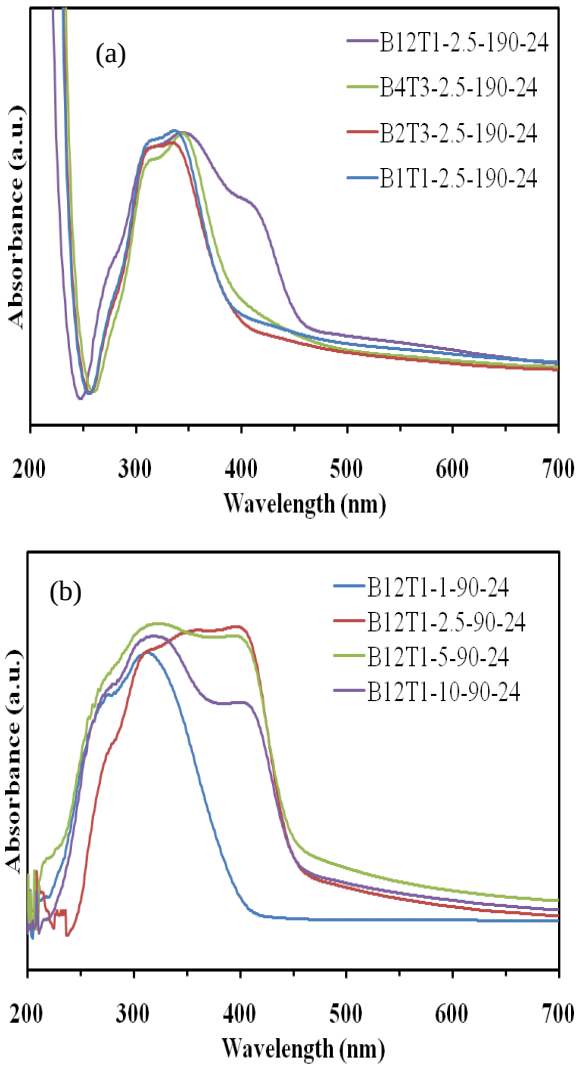

Figure 4: UV-vis absorption spectra of the prepared bismuth oxybromide catalysts. (a) Bi/Ti mole ratio; (b) NaOH concentration.

3.2 Photocatalytic Activity Evaluation

The photocatalytic performances of the bismuth titanate catalysts were evaluated by degrading AB1 under visible light or UV irradiation with 0.5 g/L of catalyst added. The degradation efficiencies as a function of reaction time are illustrated in Figure 5. Figure 5 (a) shows the results for the photodegradation of AB1 under visible light irradiation with the bismuth titanate material. It was clear that the concentration of AB1 decreased faster for the B12T1-2.5-190-24, indicating a higher photocatalytic activity for the B12T1-2.5-190-24. The improved photocatalytic performance of the B12T1-2.5-190-24 was attributed to the amount of Bi incorporated in the bismuth titanate, providing more active sites for the photocatalytic reaction and promoting the efficiency of the electron–hole separation due to high crystallinity. As shown in Figure 5 (b), the photocatalytic activity on the NaOH concentration was studied. This result indicated that the bismuth titanate by 10 M NaOH could improve the photocatalytic activity. However, the best conversion was obtained when the B12T1-10-90-24 was used because of its surface structure. The Bi on the B12T1-10-90-24 surface might increase the surface area to generate more O- radicals derived from hydroxyl groups adsorbing on the B12T1-10-90-24 surface. These O- radicals could bleach AB1 by attacking S atom of AB1 [12]. Moreover, the Bi could inhibit the recombination probability of electron-hole pairs because the photogenerated electrons transferred to the bismuth titanate surface more easily by a shorter pathway.

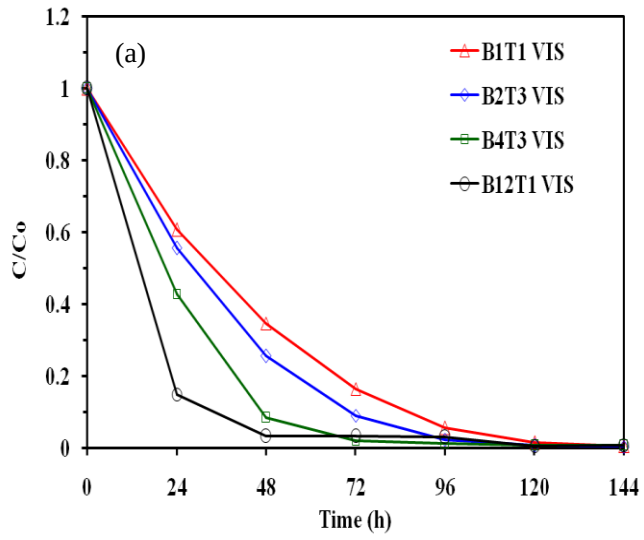

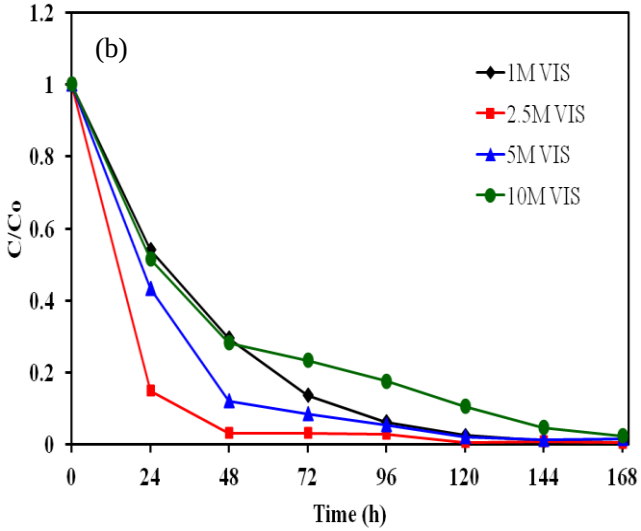

Figure 5: Photocatalytic degradation of AB1 by the resulting bismuth titanate catalysts and the control experiments under simulated visible light irradiation. (a) Bi/Ti mole ratio; (b) NaOH concentration.

4 Conclusion

We provide a new and facile way to prepare bismuth titanate in aqueous solution. The as-prepared bismuth titanate shows high photocatalytic activity for the degradation of organic dye AB1 under visible light. It is a potential strategy to fabricate novel photocatalysts for the degradation of organic pollutants in the wastewater. This work will be valuable for the practical application of the synthesized photocatalysts, and also help understand the factors in the photocatalytic activity for this kind of system.

Acknowledgments

This research was supported by the National Science Council of the Republic of China.

References

[1] C. Euvananont, C. Junin, K. Inpor, P. Limthongkul, C. Thanachayanont. *Ceram. Int.*, **34**, pp. 1067-1071, 2008.

[2] R. Dholam, N. Patel, M. Adami, A. Miotello. *Int. J. Hydrogen Energ.*, **33**, pp. 6896-6903, 2008.

[3] J. Chen, J. Zhang, Y. Xian, X. Ying, M. Liu, L. Jin. *Water Res.*, **39**, pp. 1340-1346, 2005.

[4] Y. Bessekhouad, D. Robert, J. Weber. *Catal. Today*, **101**, pp. 315-321, 2005.

[5] M. Shang, W. Wang, L. Zhang, S. Sun, L. Wang, L. Zhou. *J. Phys. Chem. C*, **113**, pp. 14727-14731, 2009.

[6] J. K. Zhou, Z. G. Zou, A. K. Ray, X. S. Zhao. *Ind. Eng. Chem. Res.*, **46**, pp. 745-749, 2007.

[7] M. Shang, W.Z. Wang, S.M. Sun, L. Zhou, L. Zhang. *J. Phys. Chem. C*, **112**, pp. 10407-10411, 2008.

[8] W. Yao, H. Wang, X. Xu, X. Cheng, J. Huang, S. Shang, X. Yang, M. Wang. *Appl. Catal. A*, **243**, pp. 185-190, 2003.

[9] M. T. Buscaglia, M. Sennour, V. Buscaglia, C. Bottino, V. Kalyani, P. Nanni. *Cryst. Growth Des.*, **l**, pp. 1394-1401, 2011.

[10] J. G Hou, Z. Wang, S. Q Jiao, H. G Zhu. *J. Hazard. Mater.*, **192**, pp.1772-1779, 2011.

[11] Y. H Shi, C. S. Cao, S. H. Feng. *Mater. Lett.*, **46**, pp. 270-273, 2000.

[12] A. Houas, H. Lachheb, M. Ksibi, E. Elaloui, C. Guillard, J.M. Herrmann. *Appl. Catal. B*, **31**, pp. 145-157, 2001.